

## Rotators for the Hadron Storage Ring

K. Hock

February 2026

Electron-Ion Collider  
**Brookhaven National Laboratory**

**U.S. Department of Energy**  
USDOE Office of Science (SC), Nuclear Physics (NP)

Notice: This technical note has been authored by employees of Brookhaven Science Associates, LLC under Contract No. with the U.S. Department of Energy. The publisher by accepting the technical note for publication acknowledges that the United States Government retains a non-exclusive, paid-up, irrevocable, world-wide license to publish or reproduce the published form of this technical note, or allow others to do so, for United States Government purposes.

## **DISCLAIMER**

This report was prepared as an account of work sponsored by an agency of the United States Government. Neither the United States Government nor any agency thereof, nor any of their employees, nor any of their contractors, subcontractors, or their employees, makes any warranty, express or implied, or assumes any legal liability or responsibility for the accuracy, completeness, or any third party's use or the results of such use of any information, apparatus, product, or process disclosed, or represents that its use would not infringe privately owned rights. Reference herein to any specific commercial product, process, or service by trade name, trademark, manufacturer, or otherwise, does not necessarily constitute or imply its endorsement, recommendation, or favoring by the United States Government or any agency thereof or its contractors or subcontractors. The views and opinions of authors expressed herein do not necessarily state or reflect those of the United States Government or any agency thereof.

# Rotators for the Hadron Storage Ring

Kiel Hock, Vadim Ptitsyn

February 27, 2026

## Abstract

The Electron Ion Collider calls for collisions of polarized electrons on transversely and longitudinally polarized protons and helions. To facilitate longitudinal polarization, helical dipole rotator magnets from the Relativistic Heavy Ion Collider will be reused. These rotators are placed asymmetrically at  $-35.28$  and  $61.35$  mrad from the interaction point. Longitudinal polarization of polarized protons cannot be satisfied for all energies while remaining below the maximum current of 322 A. Care has been taken to ensure longitudinal polarization can be satisfied at the energies of interest. The rotators ramping result in a shift in  $\nu_s$  which has been compensated for with a change in the snake precession axes. The rotators can satisfy longitudinal polarization at all energies of interest, and the  $\nu_s$  compensation has also been established.

# Introduction

The Electron Ion Collider (EIC) Hadron Storage Ring (HSR) will be primarily constructed using existing components from the Relativistic Heavy Ion Collider (RHIC). The HSR will have rotator magnets outside of the interaction regions to facilitate longitudinal or radially outward polarization at the interaction point (IP).

The helical dipoles have a period  $\lambda=2.4$  m. The magnet period is defined as [1]

$$k = H \frac{2\pi}{\lambda} \quad (1)$$

with H being the helicity (that is -1 for LH and +1 for RH). The spin rotation from one coil is,

$$\phi = 2\pi\sqrt{1 + \chi^2} \quad (2)$$

and

$$\chi = (G + 1/\gamma) \frac{qB_o}{m\beta c|k|} \quad (3)$$

where G is the anomalous gyromagnetic g-factor,  $\gamma$  is the Lorentz factor, q and m are the charge and mass,  $\beta c$  is the velocity, and  $B_o$  is the magnetic field. The maximum  $B_o = 4$  T which corresponds to a PS current of 322 A. The relevant parameters for protons and helions are found in Tab. 1.

Table 1: Relevant parameters for polarized protons and polarized helions.

	G	q	m (GeV/c <sup>2</sup> )
proton	1.7928474	1	0.93827209
helion	-4.1841536	2	2.80839148

The rotation from a single helix occurs in the laboratory frame about the precession axis defined as,

$$u = \left[ -\frac{\chi}{\sqrt{1 + \chi^2}}, -\frac{H}{\sqrt{1 + \chi^2}}, 0 \right]. \quad (4)$$

The full rotator assembly consists of four helical dipoles. After transiting the full rotator assembly, the spin has been placed in the horizontal plane. The residual angle from the horizontal plane is  $\theta_y = 0$ . After this spin has been placed in the horizontal plane, it will precess by an amount  $\theta_s$ , defined as

$$\theta_s = G\gamma\theta_R \quad (5)$$

where  $\theta_R$  is the bend angle from the IP to the rotator.

The existing RHIC rotators have a helicity pattern of RLRL. These magnets are powered similar to the snakes where the inner and outer coils are powered independently with current  $I_{in}$  and  $I_{out}$ , but all coils have the same sign for current, such as R+L+R+L+ [2]. The RHIC rotators are placed symmetrically on either side of the IP with an angle of  $\theta_R = \pm 3.675$  mrad from the IP. These rotator assemblies will be used for the HSR. In the HSR, the stored beam circulates in the counter-clockwise direction, equivalent to the yellow RHIC ring. Thus, the sector 6 rotator is to be the V2H (vertical to horizontal) rotator, and the sector 5 snake is the H2V (horizontal to vertical). This document builds on previously reported results from [3].

## Proton Configurations

Calculations using the field maps to determine the current required at a given energy are shown in Fig. 1, with markers at energies of interest (41, 100, 130, 255, and 275 GeV). Due to the PS limit of 322 A, there are energies where longitudinal polarization cannot be satisfied, a void [3]. In Fig. 1, the voids are shown as grayed areas. Due to the asymmetric  $\theta_R$  between the rotators, the  $\theta_R = 61.35$  mrad voids are 1.74X more frequent but 0.58x smaller than the  $\theta_R = -35.28$  mrad voids. Note that in this configuration, longitudinal polarization can be satisfied at 41, 100, and 275 GeV. Also, the H2V rotator is in the LRLR helicity pattern. By comparison with Fig. 2, if the H2V rotator was in the RLRL configuration, 41 GeV would coincide with one of these voids and longitudinal polarization could not be realized. This rotator must be reconfigured to the LRLR helicity pattern.

A summary of inner and outer rotator currents for the sector 5 and 6 rotators at 41, 100, and 275 GeV is found in Tab. 2. The resulting fields and trajectories are found in A.1.

## Rotator Ramp and $\nu_s$ compensation

Due to the asymmetric placement of the rotators, the spin rotation on either side of the IP will not cancel, resulting in a spin tune shift of  $\Delta\nu_s$ . The allowed operational current ramp has a maximum ramp rate of 0.47 A/s so a 264 A setpoint means the

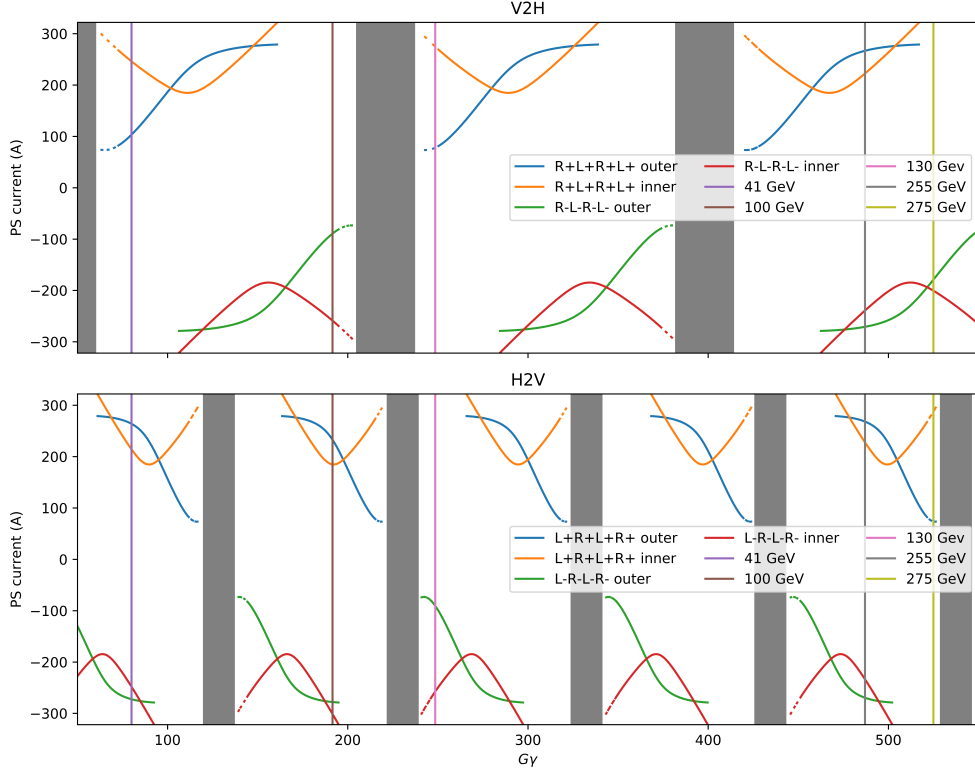


Figure 1: Inner and outer power supply currents for the sector 6 (top) and sector 5 (bottom) rotators to satisfy longitudinal polarization of protons, from  $G\gamma=50$  to 550.

Table 2: Summary of rotator configurations for protons at 41, 100, and 275 GeV.

Energy	$G\gamma$	$G\gamma\theta_{1\rightarrow IP}$	$G\gamma\theta_{IP\rightarrow 2}$	$I_{out,ROT1}$	$I_{in,ROT1}$	$I_{out,ROT2}$	$I_{in,ROT2}$
41	78.3	2.762	4.804	104	246	264	215
100	191.5	6.756	11.75	-90	-259	235	185
275	525.5	18.54	32.24	-184	-198	75	282

current ramp for all currents will take approximately 9.5 minutes [4]. Here, the compensation is defined as the change of the precession axis angle,  $\Delta\theta_{s,x}$  [2]. Fig. 3 shows  $\nu_s$  with and without compensation as a function of rotator scaling, and the associated compensation schemes with multiple snake axes for compensation. The change in the snake PS currents for the single snake compensation case is found in Fig. 4. As seen in the right plot, as long as the axis change is in the negative direction, there is sufficient current to compensate it, as long as the axis does not go negative. If it is required that the axis change is to go negative, there is no

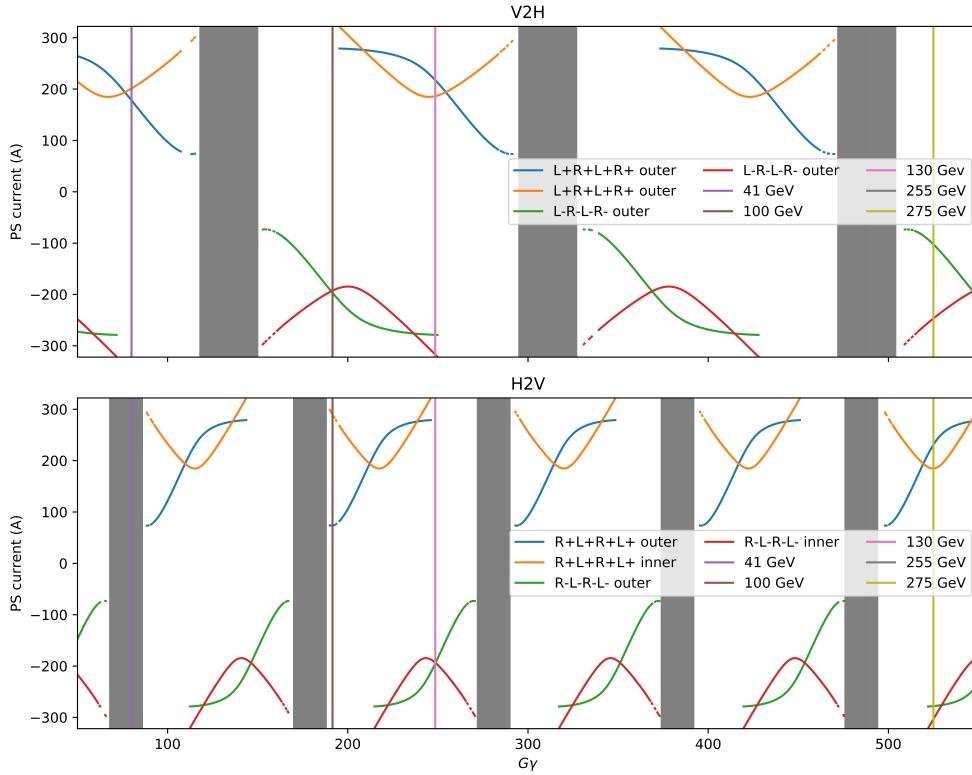


Figure 2: Alternate helicity for the two rotator modules, inner and outer power supply currents for the sector 6 (top) and sector 5 (bottom) rotators to satisfy longitudinal polarization of protons, from  $G\gamma=50$  to 550.

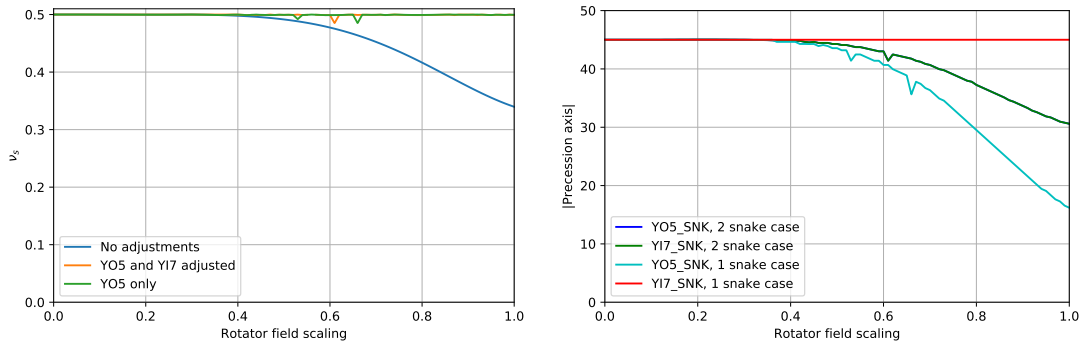


Figure 3: Left:  $\nu_s$  as a function of rotator amplitude comparing the uncompensated case, adjusting a single snake, and adjusting two snakes. Right: The resulting change in snake precession axis to maintain  $\nu_s=1/2$ .

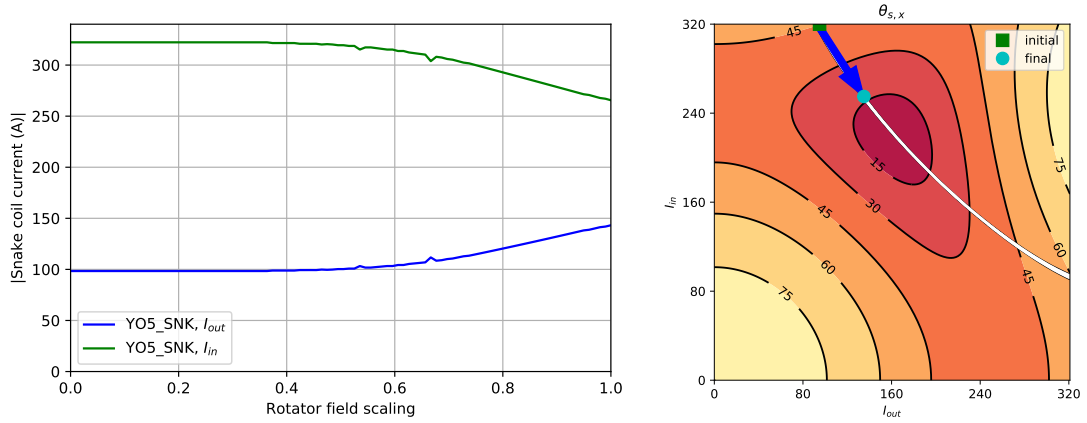


Figure 4: Left: the inner and outer snake currents to compensate the  $\Delta\nu_s$  from the rotator ramping. Right: the trajectory of the current from its initial to final precession axis.

solution as this would require ramping the power supplies to zero which would move the snake off of the  $180^\circ$  spin-flip line and ruin polarization. Similarly, if the axis change was above  $45^\circ$ , the initial currents would need to be at the alternate  $45^\circ$  axis which has unfavorable orbit matching requirements, and would support a maximum precession axis of  $60^\circ$ .

The summary of  $\Delta\nu_s$  and  $\Delta\theta_{s,x}$  at 41, 100, and 275 GeV are shown in Tab. 3. The  $\Delta\nu_s$  here refers to the uncompensated shift in  $\nu_s$  from the rotators ramping. Additional analysis for 41 and 100 GeV can be found in A.2.

Table 3: Summary of  $\Delta\nu_s$  from rotators ramping with protons and its compensation using the snakes at 41, 100, and 275 GeV..

Energy	$\Delta\nu_s$	Snakes used	$\Delta\theta_{s,x}$
41	0.107	1	-38.9
100	0.346	4	-20.8
275	0.169	1	-28.8

## Helion Configuration

Due to the difference in  $G$ ,  $q$ , and  $m$  of helions relative to protons, they will be rotated 1.56x more per unit field of  $B_o$ . As a result, the rotators can satisfy longitudinal polarization at all energies, as seen in Fig. 5. Tab. 4 summarizes the rotator configurations at 41, 100, and 183 GeV/u. Note that in Tab. 5, the values in ( ) denote alternate solutions.

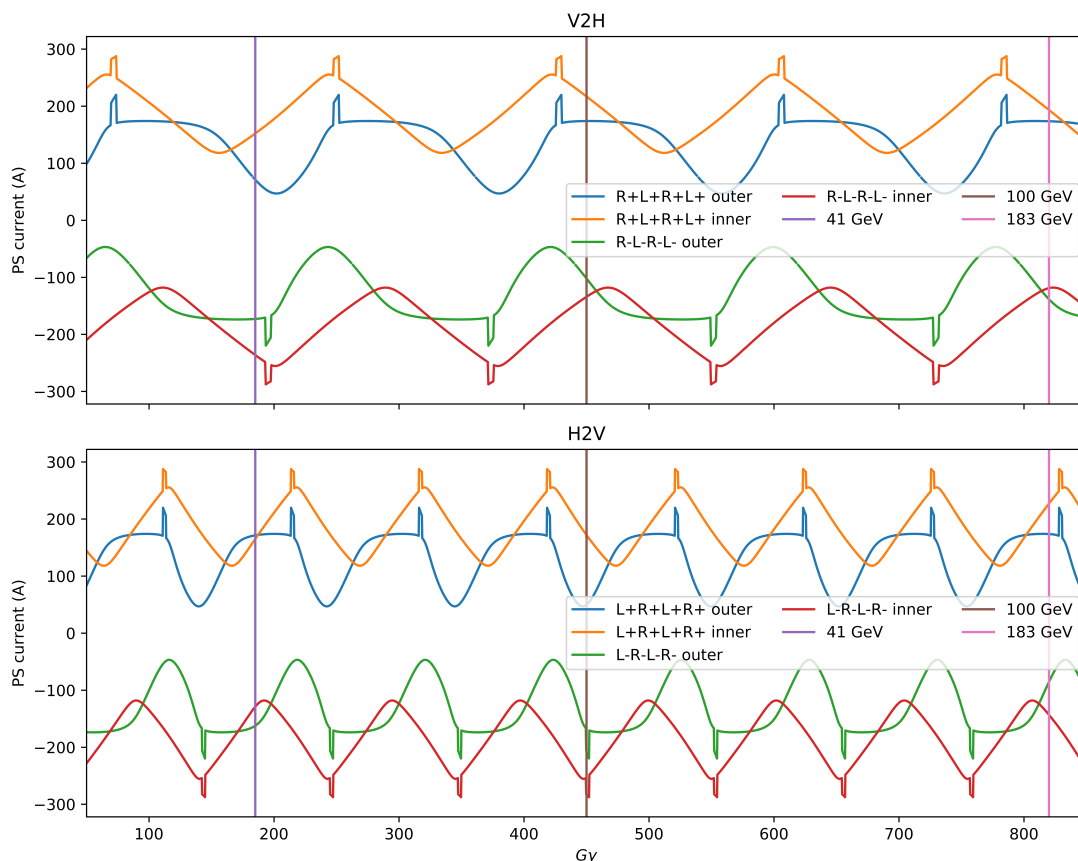


Figure 5: Rotator currents for the inner and outer power supplies for the sector 6 (top) and sector 5 (bottom) rotators for polarized helions from  $|G\gamma|=50$  to 850.

The compensation schemes are summarized in Tab. 5, and the available snake axes are shown in Fig. 6. For helion, all changes in precession axis require a positive change. This is achievable with the favorable  $45^\circ$  precession axis, as long as the total change is less than  $28^\circ$  as the maximum supported axis with  $I_{out} < I_{in}$  is  $73^\circ$ . Due to the larger  $G$ , a minimum of four snakes are required to compensate the spin-tune shift. On the side where  $I_{out} > I_{in}$ , all axes from 0 to  $180^\circ$  can be achieved.

Table 4: Summary of rotator configurations for helions at 41, 100, and 183 GeV/u.

Helion	$G\gamma$	$G\gamma\theta_{1\rightarrow IP}$	$G\gamma\theta_{IP\rightarrow 2}$	$I_{out,ROT1}$	$I_{in,ROT1}$	$I_{out,ROT2}$	$I_{in,ROT2}$
41	183.3	6.465	11.24	75(-173)	150(-234)	171(-164)	160(-133)
100	447.0	15.78	27.42	174(-94)	221(-138)	47(-157)	181(-255)
183	817.9	28.87	50.18	174(-139)	192(-119)	174(-89)	225(-141)

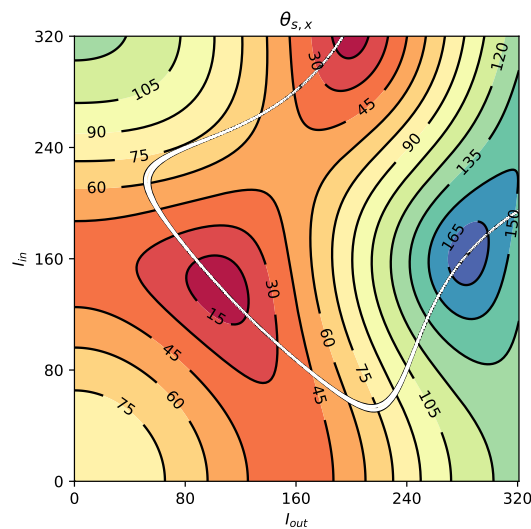


Figure 6: The plot shows the attainable snake precession axes as a function of inner and outer PS current. The white line corresponds to a  $180^\circ$  rotation.

Table 5: Summary of  $\Delta\nu_s$  from rotators ramping with helions and its compensation using the snakes.

Energy	$\Delta\nu_s$	Snakes used	$\Delta\theta_{s,x}$
41	0.392	4	+13.2
100	0.294	4	+26.4
275	0.217	4	+19.4

# Bibliography

- [1] F. Méot et al. *Polarized Beam Dynamics and Instrumentation in Particle Accelerators : USPAS Summer 2021 Spin Class Lectures*. Springer, 2023.
- [2] K. Hock and V. Ptitsyn. *Snakes for the Hadron Storage Ring*. Snakes for the Hadron Storage Ring: EIC-ADD-TN-141, 2025.
- [3] Vadim Ptitsyn and J. Berg. EIC Hadron Spin Rotators. *JACoW, IPAC2022: WEPOST020*, 2022. doi: 10.18429/JACoW-IPAC2022-WEPOST020.
- [4] RHIC PS group. *MCR Snake and Spin Rotator Power Supply Instructions 2/14/22*, 2022. <https://www.cadops.bnl.gov/RHIC/PSGroup/PSGroupWiki-1.39.7/images/4/42/MCRSnakeMagInstructions2x14x22.pdf>.

# Appendix A

## Appendix

### A.1 Trajectories

#### A.1.1 Protons

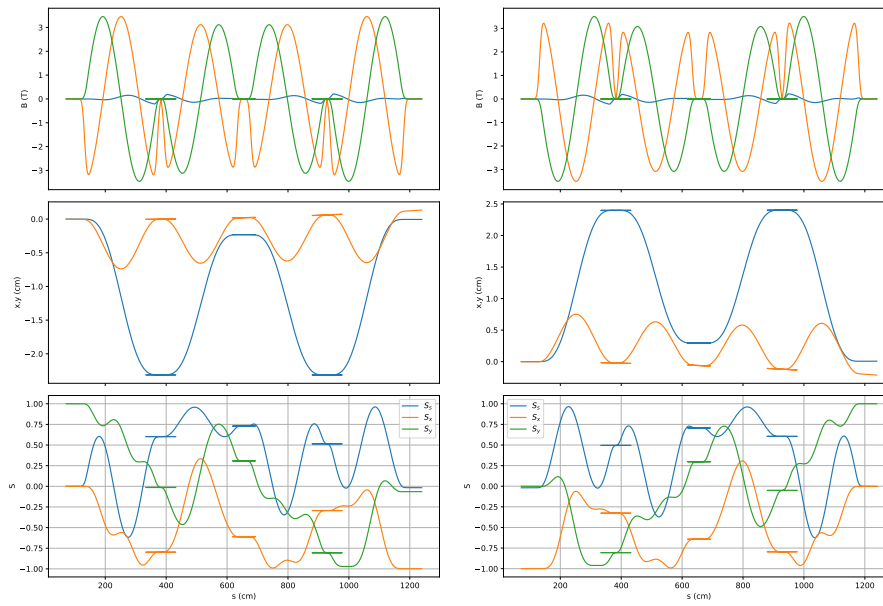


Figure A.1: Protons 41 GeV

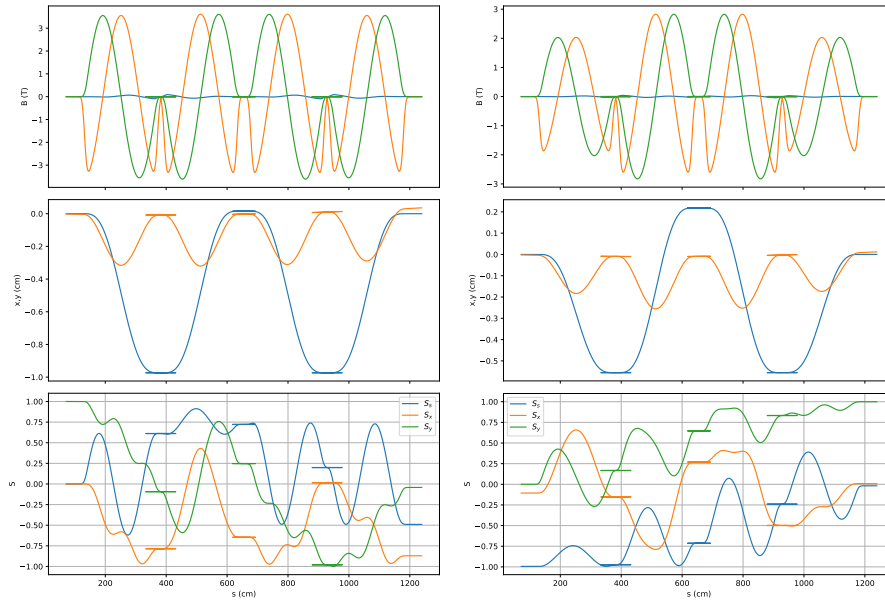


Figure A.2: Protons 100 GeV

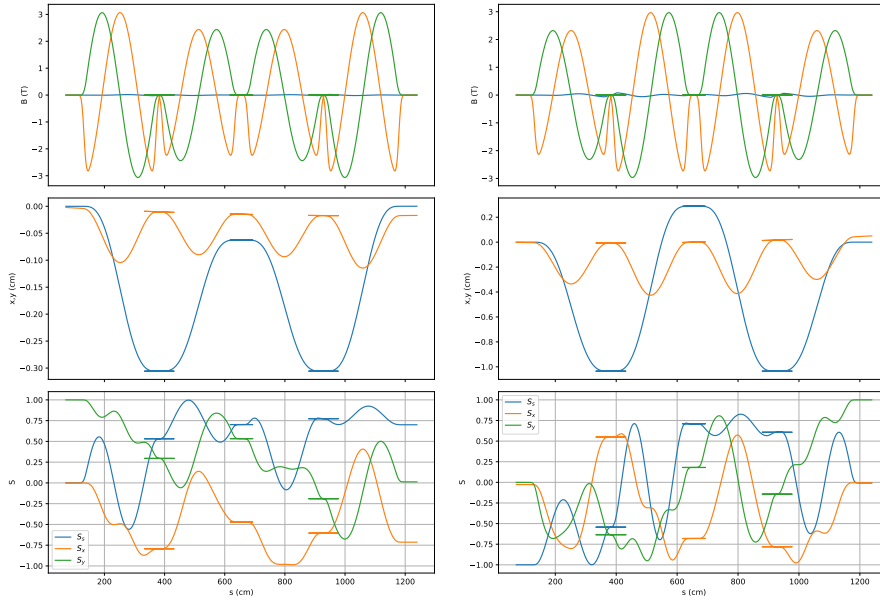


Figure A.3: Protons 275 GeV

## A.1.2 Helions

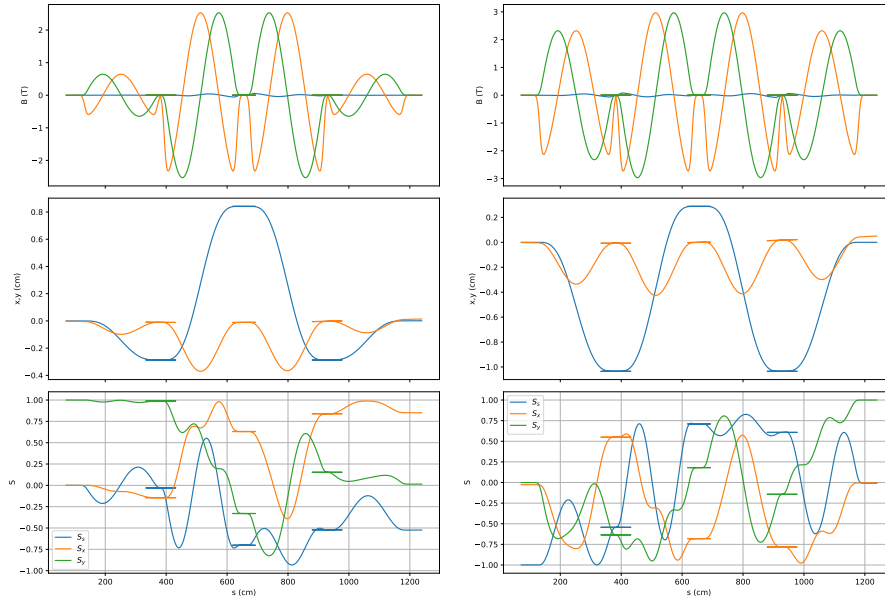


Figure A.4: Helions 41 GeV/u

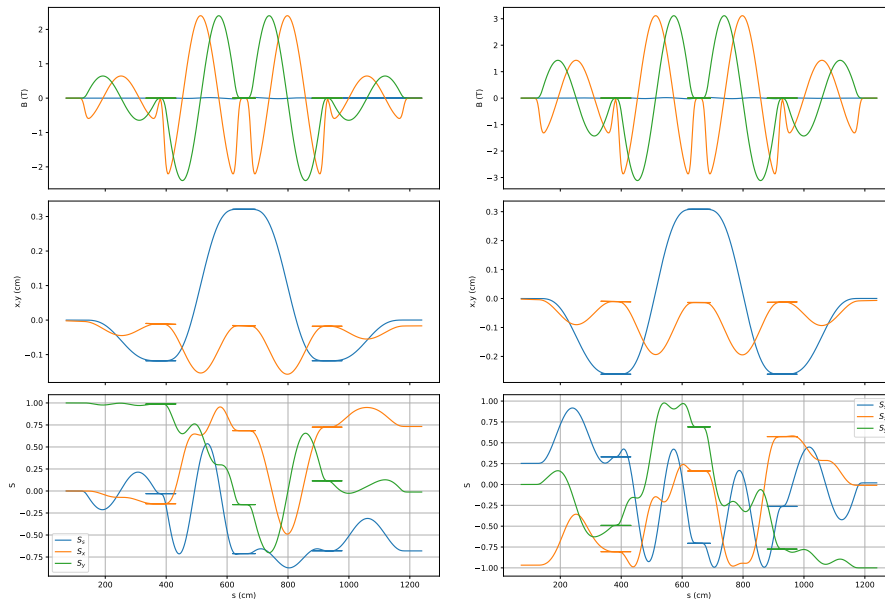


Figure A.5: Helions 100 GeV/u

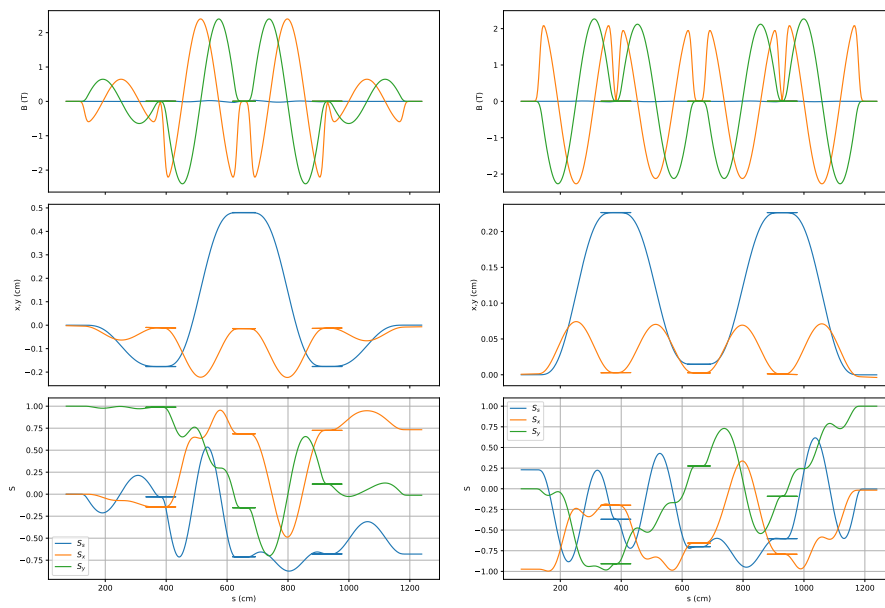


Figure A.6: Helions 183 GeV/u

## A.2 $\nu_s$ compensation

### A.2.1 Protons

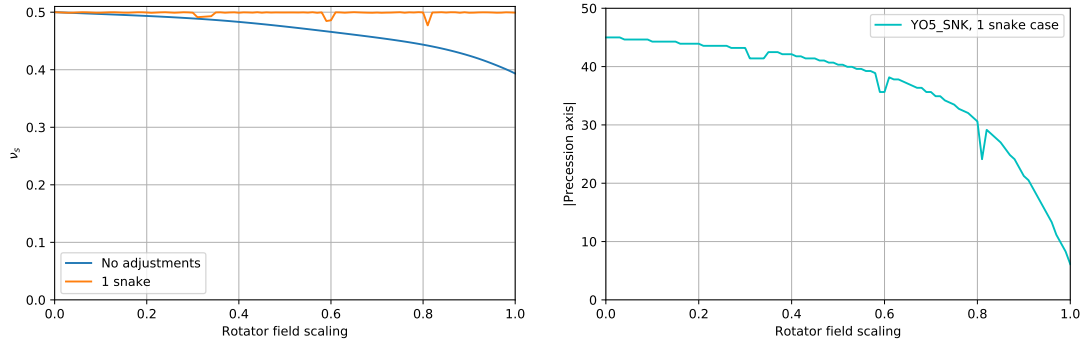


Figure A.7:  $\Delta\nu_s$  and  $\Delta\theta_{s,x}$  compensation for different snake configurations of protons at 41 GeV.

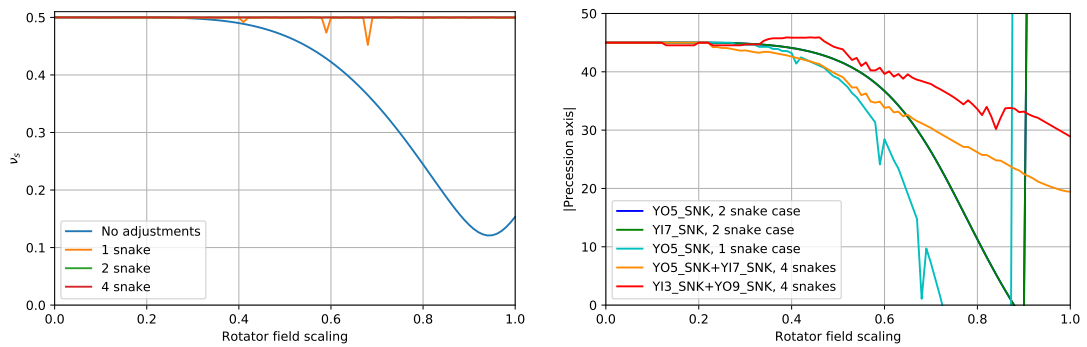


Figure A.8:  $\Delta\nu_s$  and  $\Delta\theta_{s,x}$  compensation for different snake configurations of protons at 100 GeV.

## A.2.2 Helions

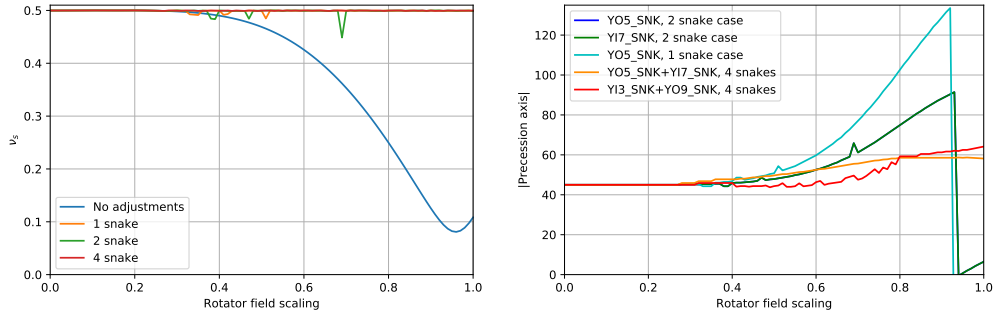


Figure A.9:  $\Delta\nu_s$  and  $\Delta\theta_{s,x}$  compensation for different snake configurations of helions at 41 GeV/u.

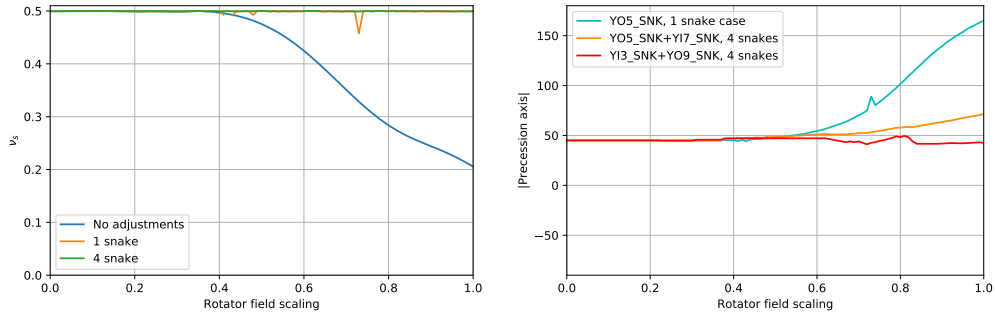


Figure A.10:  $\Delta\nu_s$  and  $\Delta\theta_{s,x}$  compensation for different snake configurations of helions at 100 GeV/u.

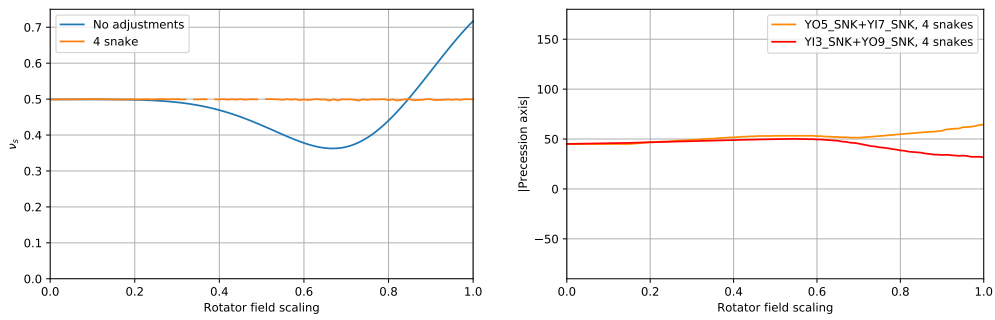


Figure A.11:  $\Delta\nu_s$  and  $\Delta\theta_{s,x}$  compensation for different snake configurations of helions at 183 GeV/u.